Fusion Engineering and Design 89 (2014) 1595–1599

Contents lists available at ScienceDirect

Fusion Engineering and Design

journal homepage: www.elsevier.com/locate/fusengdes

# Physical properties of F82H for fusion blanket design

Takanori Hirose[a,*], Takashi Nozawa[b], R.E. Stoller[c], Dai Hamaguchi[b], Hideo Sakasegawa[b], Hiroyasu Tanigawa[b], Hisashi Tanigawa[a], Mikio Enoeda[a], Yutai Katoh[c], L.L. Snead[c]

[a] Japan Atomic Energy Agency, Naka, Ibaraki, Japan
[b] Japan Atomic Energy Agency, Rokkasho, Aomori, Japan
[c] Oak Ridge National Laboratory, Oak Ridge, Tennessee, United States

## HIGHLIGHTS

- Empirical equations of physical properties of F82H were defined.
- Most of physical properties of F82H superiors to Grade 91.
- Slight irradiation effects on thermal expansion and electrical resistivity of F82H.

## ARTICLE INFO

*Article history:*
Received 9 September 2013
Received in revised form
23 November 2013
Accepted 5 December 2013
Available online 18 January 2014

*Keywords:*
Reduced activation ferritic/martensitic steel
Breeding blanket
Physical properties
Numerical analysis

## ABSTRACT

The material properties, focusing on the properties used for design analysis were re-assessed and newly investigated for various heats of reduced activation ferritic/martensitic steel, F82H. Moreover, irradiation effects on those properties were studied in this work. Most of physical properties of unirradiated F82H are insensitive to the heat-to-heat variation, and more preferable to Grade 91 specified in the ASME code. Therefore numerical analysis using data of Grade 91 can be a conservative evaluation for F82H. The change in these properties of F82H is less than 6%. Therefore the irradiation effects on thermal stress and variation of electromagnetic force in plasma disruption could be quite small in the irradiation conditions studied.



## 1. Introduction

The most promising structural material for fusion blankets, reduced activation ferritic martensitic (RAF/M) steel is a kind of martensitic heat-resistant steel. A RAF/M, F82H has been developed to reduce induced radioactivity from 9%-Cr steel (Grade 91) by replacing and/or eliminating harmful elements such as molybdenum, niobium, nickel, and so on [1]. Although the mechanical properties of F82H generally surpass those of Grade 91, F82H has not been listed on any structural codes. The mechanical loads acting on the blanket module are categorized to thermal loads, pressure of coolant and electromagnetic forces. Considering the structural integrity of the blanket module, these loads should be verified. In the design analysis of the blanket modules, the stress is calculated from the physical properties of structural materials then the geometries are modified so that the stress is lower than the allowable stress specified in the structural codes. In a fusion reactor environment, no reduction of the allowable stress of RAF/M due to the irradiation effects emerges except for irradiation creep [2,3]. On the other hand, the loads acting on the blanket might be increased due to irradiation effects on the physical properties. However, the physical properties reported on F82H are limited to the data obtained from a single heat, so called F82H-IEA [4].

Therefore, the material properties, focusing on the properties used for design analysis were re-assessed and newly investigated for various heats including F82H-IEA. The properties were compared with grade 91 listed on ASME and Eurofer listed on RCC-MRx [1,5]. Moreover, the irradiation effects on those properties were studied in this work.

## 2. Experimental procedure

### 2.1. Materials used

The chemical compositions of the materials used in this work are summarized in Table 1. F82H-IEA was prepared for the IEA

* Corresponding author at: 801-1 Mukoyama, Naka, Ibaraki 311-0193, Japan. Tel.: +81 29 270 7516; fax: +81 29 270 7489.
*E-mail address:* hirose.takanori@jaea.go.jp (T. Hirose).

0920-3796/$ – see front matter © 2013 Elsevier B.V. All rights reserved.
http://dx.doi.org/10.1016/j.fusengdes.2013.12.005

**Table 1**
Chemical compositions of F82H used in this work (wt.%).

| | C | Si | Mn | Cr |
|---|---|---|---|---|
| F82H IEA | 0.09 | 0.07 | 0.10 | 7.84 |
| F82H BLK | 0.08 | 0.10 | 0.49 | 7.38 |
| F82H BA07 | 0.09 | 0.17 | 0.46 | 8.00 |
| F82H mod3 | 0.10 | 0.10 | 0.13 | 8.16 |
| TIG weldment | 0.05 | 0.11 | 0.40 | 7.61 |

| | W | V | Ta | N |
|---|---|---|---|---|
| F82H IEA | 1.98 | 0.19 | 0.04 | 0.007 |
| F82H BLK | 2.04 | 0.22 | 0.026 | 0.0064 |
| F82H BA07 | 1.88 | 0.19 | 0.03 | 0.019 |
| F82H mod3 | 1.94 | 0.20 | 0.09 | 0.0014 |
| TIG weldment | 1.92 | 0.19 | 0.02 | 0.0156 |

round robin tests and its physical properties have been reported [4]. F82H-BLK was 5000 kg heat produced in Vacuum Induction Melting, VIM process, which is same as F82H-IEA [6]. F82H-BA07 was molten in VIM followed by Electro-Slag-Remelting, ESR process as a secondary refinement [7]. F82H-mod3 is toughness-improved F82H with additional tantalum [8]. Weldment from TIG joint of 25 mm thickness was also investigated in this work [9].

### 2.2. Neutron irradiation

Neutron irradiation was conducted in the High Flux Isotope Reactor (HFIR) at the Oak Ridge National Laboratory (ORNL). The specimens were irradiated in molten lithium using the instrumented capsule MFE-RB-15J, which had an europium thermal neutron shield for neutron spectrum tailoring. Irradiation temperature was determined by nuclear heating of specimens and monitored using thermocouples inserted at the centerline of each sub-capsule. The nominal irradiation temperatures are 573 and 673 K. Further information on the irradiation experiment can be found elsewhere [10].

### 2.3. Measurements of physical properties

Elastic modulus, modulus of rigidity and Poisson ratio were measured on $\phi$16 mm × 10 mm rod using RITEC RAM-5000 in accordance with Japan Industrial Standard, JIS Z2280. Specific heat was measured at the temperatures between room temperature and 1173 K using differential scanning calorimeter in accordance with JIS R1672. Thermal diffusivity was calculated by half-time method using laser flash method in accordance with JIS R1611. Thermal conductivity was calculated from these and density evaluated by Archimedes' principle in accordance with JIS Z8807.

Coefficient of thermal expansion (CTE) was measured on $\phi$5 mm × 20 mm rod following the guidelines in ASTM E 831-06. For post-irradiation measurements, coupon specimens with dimensions of 4 mm × 16 mm × 0.5 mm were employed for the dilatometer, DIL402CD Netzsch-GmBH [11]. Magnetic property measurements were carried out on $\phi$3 mm × 7 mm rods cut out from a plate of F82H-BLK. The longitudinal direction is parallel to the rolling direction. DMS vibrating specimen magnetization measurement machine (VSM) was employed to obtain hysteresis loop at the temperature between 293 K and 973 K. Electrical resistivity was measured on $\phi$3 mm × 80 mm rod using a four-point probe technique following the guidelines in ASTM B 193-02. SS-J3 sheet tensile specimens with gauge dimensions of 5 mm × 1.2 mm × 0.76 mm were also used for post-irradiation measurements at room temperature.

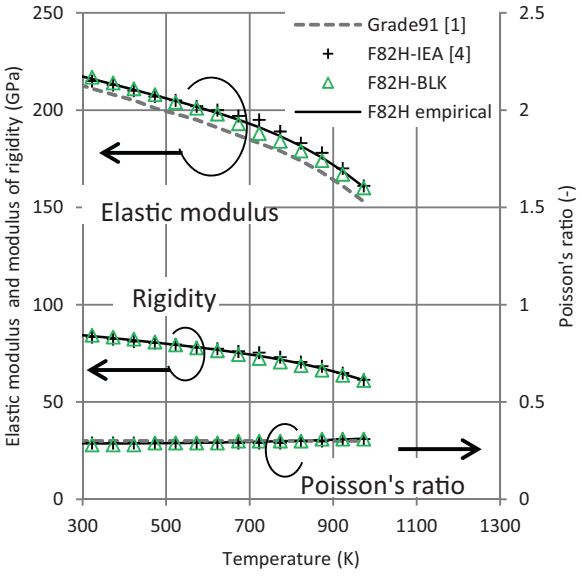


**Fig. 1.** Elastic properties of unirradiated F82H.

## 3. Results

### 3.1. Elastic properties

Elastic modulus, modulus of rigidity and Poisson ratio are compared with Grade 91 steel in Fig. 1. As shown in this figure, elastic properties measured in this work are very similar to those of the published data [3]. Comparing to Grade 91, the deviation was less than 5%. Poisson's ratio of Grade 91 is specified as 0.30 for all temperature range. On the contrary, F82H shows 0.28–0.31 and slightly increases with the temperature.

### 3.2. Thermal properties

#### 3.2.1. Specific heat, thermal diffusivity and thermal conductivity

Specific heat and thermal diffusivity of F82H are shown in Figs. 2 and 3, respectively. Peaks around 1000 K in these figures correspond to phase transformation from $\alpha$ to $\gamma$. Although data

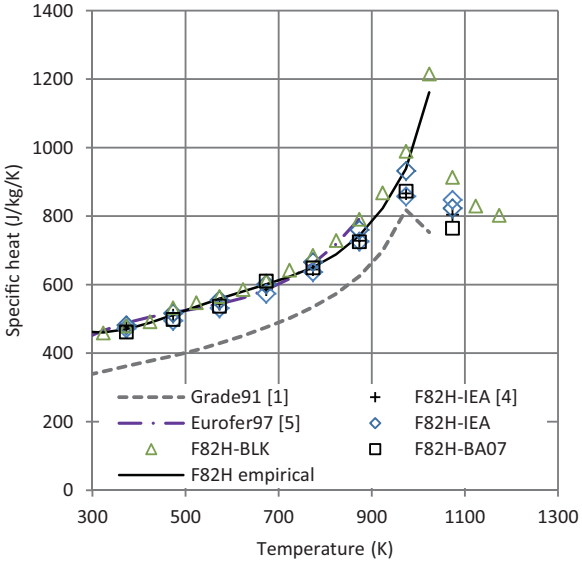


**Fig. 2.** Specific heat of unirradiated F82H.

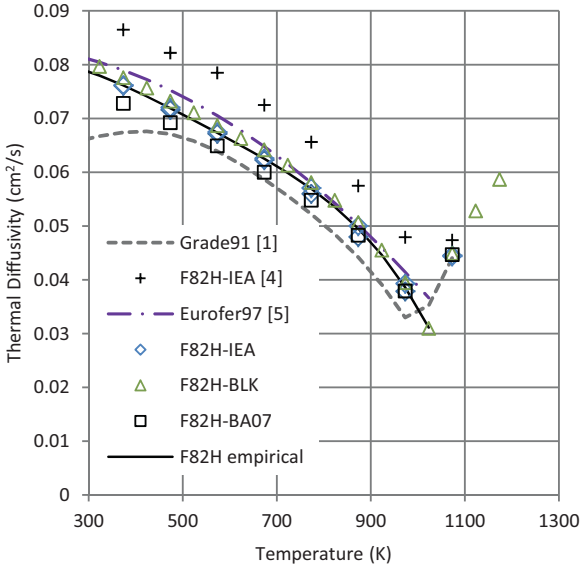


**Fig. 3.** Thermal diffusivity of unirradiated F82H.

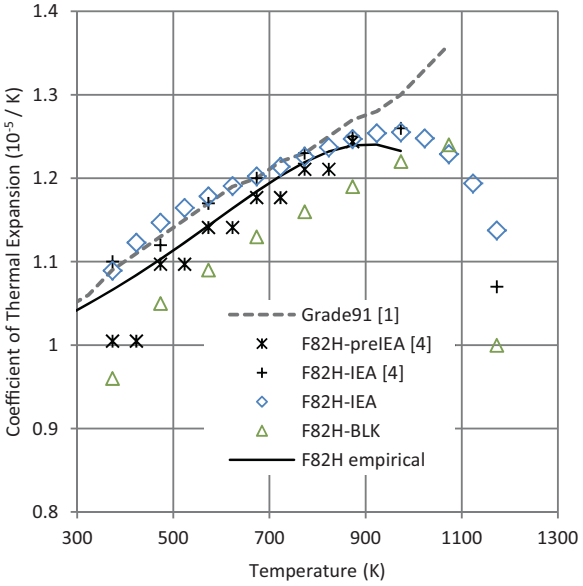


**Fig. 5.** Thermal expansion of unirradiated F82H.

scattering in specific heat is very small, the published data of the thermal diffusivity of F82H are significantly higher than the others. Excluding the published data, the thermal diffusivity at each temperature fell into ±5% of the empirical equation. Thermal conductivity of F82H derived from these empirical equations and density is presented in Fig. 4. The density of F82H-IEA, F82H-BLK and F82H-BA07 fell into $7887 \pm 0.014\,kg/m^3$ at 293 K.

### 3.2.2. Coefficient of thermal expansion

Results of CTE measurement on unirradiated F82H are presented in Fig. 5. The reference value of Grade 91 is a mean CTE [1]. The CTE at each temperature fell into ±10% of the range of the empirical equation below Ac1 temperature. The thermal expansion of F82H is very similar to that of Grade 91.

The irradiation effects on the CTE of F82H are presented in Fig. 6. Although the irradiated materials showed less CTE than the unirradiated materials in the measured temperature range, the deviation decreased with temperature above 588 K of the irradiation temperature. As shown in this figure, the irradiation effects on the CTE were quite small at this dose level.

## 3.3. Electro-magnetic properties

### 3.3.1. Magnetic properties

Magnetic properties obtained from the hysteresis loop are presented in Fig. 7. Two heats of F82H demonstrated very similar saturation magnetization. Moreover, the difference between F82H and Eurofer was less than 6%. On the contrary, large scattering with factors of 2–5 was observed in remanence magnetization.

### 3.3.2. Electrical resistivity

Results of electrical resistivity measurement on unirradiated F82H are presented in Fig. 8. The resistivity linearly increases with test temperature. No significant difference between materials was observed. F82H with 20% cold work (CW) is also plotted in this figure to evaluate dislocation effects on the resistivity. Although the CW material showed Hv harder than the normal material, the resistivity of CW was 7% larger than the normal material. Relationship between hardness change and resistivity change are presented in Fig. 9. The horizontal axis represents the hardness change induced by neutron irradiation or cold work. The vertical axis represents the resistivity change from the normal condition. Although both

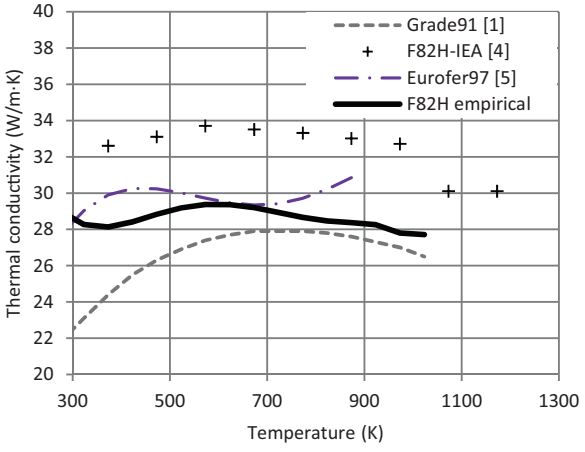


**Fig. 4.** Thermal conductivity of unirradiated F82H.

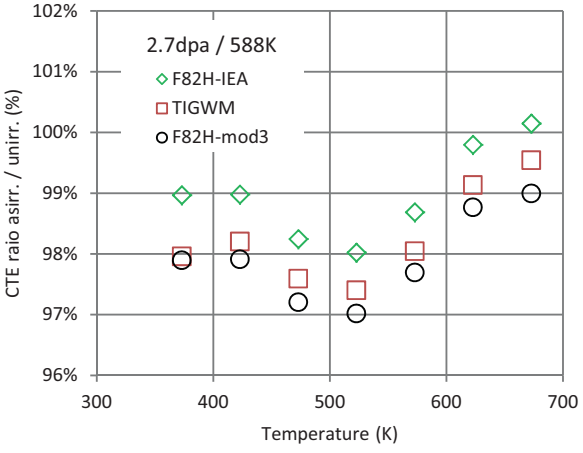


**Fig. 6.** Irradiation effects on CTE of F82H.

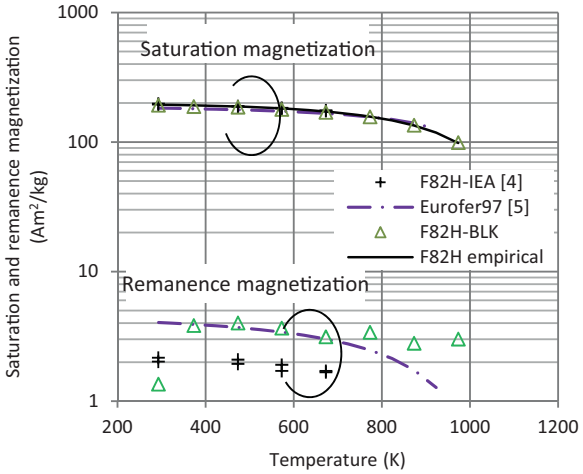


**Fig. 7.** Magnetization of unirradiated F82H.

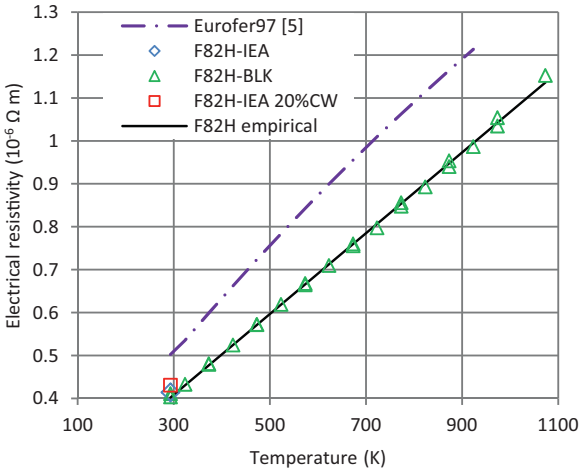


**Fig. 8.** Electrical resistivity of unirradiated F82H.

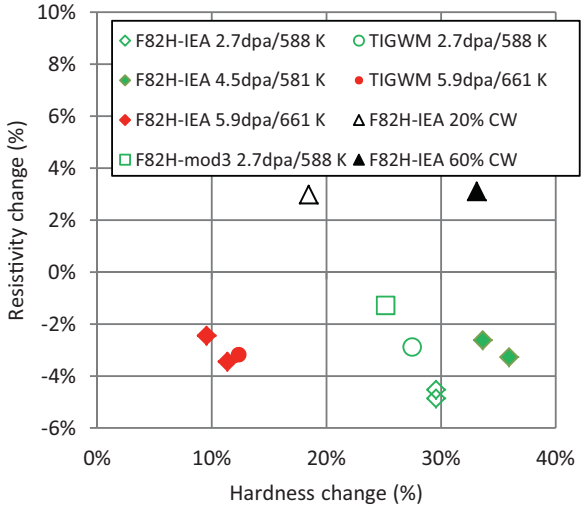


**Fig. 9.** Hardness–resistivity relationship in F82H after neutron irradiation.

neutron irradiation and cold work hardened the material, neutron irradiation reduced the resistivity but cold work increased.

## 4. Discussions

### 4.1. Unirradiated properties

Table 2 summarizes the parameters for empirical equations of unirradiated F82H physical properties.

The empirical equation is defined as

$$Y = A + B * T + C * T^2 + D * T^3 + E * T^4 \quad (1)$$

where $Y$ is physical properties at each temperature, $T$ is temperature in Kelvin from 273 K to 973 K.

As shown in Fig. 1, the elastic modulus of F82H was 3–5% higher than that of Grade 91, which stand for the average of 5–9% Cr steels belonging to Material Group E in TABLE TM-1 [1]. The elastic modulus of F82H demonstrated very similar values and temperature dependence. Therefore it might be reasonable to put on F82H to Material Group E in TABLE TM-1. As shown in Figs. 3 and 4, the published thermal conductivity of F82H-IEA is quite higher than the others due to higher thermal diffusivity. The highest diffusivity shows very similar temperature dependence to the others. Therefore it might be due to over estimation of loss of heat in the measured samples. As shown in Fig. 4, thermal conductivity of F82H is greater than that of Grade 91 and similar to that of Eurofer. According to these results, thermal properties of F82H are very similar to those of Eurofer and more preferable to Grade 91 steel because a higher thermal conductivity reduces the temperature gradient, which leads less thermal stress. Similarly, thermal expansion of F82H showed small scattering, and it is more preferable to Grade 91 steel because a less CTE leads less thermal stress. It means thermo-mechanical analysis using data of Grade 91 for F82H leads to overestimate the temperature gradient and thermal expansion of F82H.

In case of electromagnetic force analysis, electro-magnetic properties are used as input data. As shown in Figs. 7 and 8, saturation magnetization, which corresponds to the relative permeability, and electrical resistivity were insensitive to the materials. On the contrary, remanence magnetization showed large scatter. It was reported that coercive field of a steel depends on grain size and residual stress [12]. Although the impact of remanence on design analysis is not significant, it could affect the on-site weldability such as magnetic arc blow on welding.

### 4.2. Irradiation effects on physical properties

Considering thermal stress introduced in the irradiated material, it is necessary to take into account for the irradiation effects

**Table 2**
Parameters for empirical equations of unirradiated F82H physical properties.

| Properties | Unit | A | B | C | D | E |
|---|---|---|---|---|---|---|
| Elastic modulus | GPa | 2.33E+02 | −4.26E−02 | −6.34E−05 | 1.37E−07 | −1.08E−10 |
| Modulus of rigidity | GPa | 8.82E+01 | −1.27E−03 | −5.93E−05 | 8.40E−08 | −5.25E−11 |
| Specific heat | J/kg/K | 1.20E+03 | −6.24 | 1.83E−02 | −2.19E−05 | 9.64E−09 |
| Thermal diffusivity | $cm^2/s$ | 7.04E−02 | 1.19E−04 | −4.41E−07 | 5.35E−10 | −2.48E−13 |
| Coefficient of thermal expansion | $\times 10^{-5}$/K | 9.35E−01 | 5.14E−04 | −1.02E−06 | 2.02E−09 | −1.23E−12 |
| Electrical resistivity | $\times 10^{-6}\ \Omega$ m | 1.26 | 9.41E−04 | – | – | – |

on elastic modulus, CTE and thermal conductivity. It was reported that neutron irradiation increases both elastic modulus and thermal conductivity below void swelling temperature [13,14]. As shown in Fig. 6, neutron irradiation at 573 K reduced the CTE of F82H and its variants, and the magnitude of the reduction is less than 3%. Therefore it is concluded that no extra expansion is addressed by the neutron irradiation. It is necessary to evaluate post-irradiation elastic modulus and thermal conductivity for estimation of thermal stress in the irradiated materials.

As for electro-magnetic properties, it was revealed the electrical resistivity was slightly reduced by the neutron irradiation (Fig. 9). It is suggested that it makes the induction current in the blanket increased. The cold worked material showed hardening due to increase of dislocation density and rolling texture. Although neutron irradiation increases the dislocation density, no significant change of grain morphology was expected. The reduced resistivity in the irradiated materials could be caused by the other microstructural change such as irradiation induced segregation [2]. On the other hand, the resistivity of molybdenum alloy was reduced by low dose irradiation but increased with higher dose irradiation. Therefore the resistivity of F82H could be increased with high dose irradiation [15].

Although post-irradiation magnetic properties of RAF/M has received little attention, that of reactor-pressure-vessel-steel (RPVS) are intensively studied as a non-destructive inspection method [16]. It was reported that saturation magnetization of single crystal model steel is insensitive to irradiation damage [17]. Comparing to these single crystal steels, the microstructure of F82H should be more insensitive to the irradiation effects because of its tempered martensite structure which has numerous effective sinks for irradiation induced point defects [2]. Therefore, it is expected that irradiation damage does not increase the electromagnetic force in F82H.

## 5. Conclusions

The material properties, focusing on the properties used for design analysis were investigated for various heats of a reduced activation ferritic/martensitic steel, F82H. Moreover, irradiation effects on those properties were studied in this work.

Most of physical properties of F82H are insensitive to the heat-to-heat variation, and similar to those of Grade 91 specified in the ASME code.

Neutron irradiation up to several dPa hardly changed the thermal expansion and electrical resistivity.

## Acknowledgment

This research was sponsored by Japan Atomic Energy Agency and the Office of Fusion Energy Science, US Department of Energy, under contract DE-AC05-00R22725 with UT-Battelle, LLC.

## References

[1] An International code 2010 ASME Boiler & Pressure vessel code, Section II Part D, Properties Materials (2011).
[2] H. Tanigawa, R.L. Klueh, N. Hashimoto, M.A. Sokolov, Hardening mechanisms of reduced activation ferritic/martensitic steels irradiated at 300 °C, Journal of Nuclear Materials 386–388 (2009) 231–235.
[3] M. Ando, M. Li, H. Tanigawa, M.L. Grossbeck, S. Kim, T. Sawai, et al., Creep behavior of reduced activation ferritic/martensitic steels irradiated at 573 and 773 K up to 5 (dpa), Journal of Nuclear Materials 367–370 (2007) 122–126.
[4] K. Shiba, A. Hishinuma, A. Tohyama, K. Masamura, JAERI-Tech 97-038.
[5] K. Mergia, N. Boukos, Structural, thermal, electrical and magnetic properties of Eurofer 97 steel, Journal of Nuclear Materials 373 (2008) 1–8.
[6] M. Oda, T. Kurasawa, T. Kuroda, T. Hatano, H. Takatsu, JAERI-Tech 97-013.
[7] H. Tanigawa, K. Shiba, H. Sakasegawa, T. Hirose, S. Jitsukawa, Technical issues related to the development of reduced-activation ferritic/martensitic steels as structural materials for a fusion blanket system, Fusion Engineering and Design 86 (2011) 2549–2552.
[8] K. Shiba, H. Tanigawa, T. Hirose, T. Nakata, Development of the toughness-improved reduced-activation F82H steel for demo reactor, Fusion Science and Technology 62 (2012) 145–149.
[9] T. Sawai, K. Shiba, A. Hishinuma, Microstructure of welded and thermal-aged low activation steel F82H IEA heat, Journal of Nuclear Materials 283–287 (2000) 657–661.
[10] J.L. McDuffee, D.W. Heatherly, Operating conditions and irradiation history for experiment MFE-RB-15J, DOE/ER-0313 Semi-Annual Progress Reports 49 (2010) 110–114.
[11] T. Hirose, N. Okubo, H. Tanigawa, Y. Katoh, A.M. Clark, J.L. McDuffee, et al., Irradiation temperature determination of HFIR target capsules using dilatometric analysis of silicon carbide monitors, DOE/ER-0313 Semi-Annual Progress Reports 49 (2010) 94–99.
[12] M. Chiba, M. Kaiso, Soft magnetic iron wire, Kobe Steel Engineering Reports 52 (3) (2002) 66–69.
[13] R. Kasada, H. Ono, H. Sakasegawa, T. Hirose, A. Kimura, A. Kohyama, Enhancement of irradiation hardening by nickel addition in the reduced-activation 9Cr–2W martensitic steel, Journal of Nuclear Materials 258-263 (1998) 1199–1203.
[14] R.K. Williams, R.K. Nanstad, R.S. Graves, R.G. Berggren, Irradiation effects on thermal conductivity of a light–water reactor pressure vessel steel, Journal of Nuclear Materials 115 (1983) 211–215.
[15] B.V. Cockeram, J.L. Hollenbeck, L.L. Snead, Hardness and electrical resistivity of molybdenum in the post-irradiated and annealed conditions, Journal of Nuclear Materials 336 (2005) 299–313.
[16] S. Kobayashi, T. Yamamoto, D. Klingensmith, G.R. Odette, H. Kikuchi, Y. Kamada, Magnetic evaluation of irradiation hardening in A533B reactor pressure vessel steels: magnetic hysteresis measurements and the model analysis, Journal of Nuclear Materials 422 (2012) 158–162.
[17] Y. Kamada, H. Watanabe, S. Mitani, J.N. Mohapatra, H. Kikuchi, S. Kobayashi, et al., Ion-irradiation enhancement of materials degradation in Fe–Cr single crystals detected by magnetic technique, Journal of Nuclear Materials (2013), http://dx.doi.org/10.1016/j.jnucmat.2012.11.042.